# The Effect of Equivalence Ratios Variation on Gas Turbine Fuel Types During Combustion Instabilities.

Wilson Alli, Osagie Ighodalo, Christopher Ajuwa

**Abstract**— The study is set to determine the impact and contribution of Equivalence ratio variation on gas turbine fuel types during combustion instabilities occurrence in GTE-LP Combustors. The computational fluid dynamics (CFD) technology with the ANSYS Fluent Code (Academic Research CFD) version 16.2 was adopted to conduct the direct numerical simulation (DNS) processes with the aim of investigating the effect of Equivalence ratios variation on gas turbine engine types during combustion instabilities. Four conventional gas turbine engine fuels (Automotive Gas Oil (AGO), Hydrogen gas, Dual Purpose Kerosene (DPK) and Methane/Natural gas) were selected for investigation. An AutoCAD pre-designed combustor was exported to the ANSYS Fluent GUI for fine tuning, gridding/mesh generation and discretisation with the fluent solver leveraging the finite difference method (FDM) to solve emerging complex equations. With established boundary conditions contiguous to an operational industrial gas turbine engine generating at 20MW, various fuel-air relational ratios were determined with simulations conducted under four Equivalence ratios (0.3,0.5,0.7 and 0.9)Ø in both the steady-state and transient combustions regimes for every fuel on convergence attainment to establish each fuel overall combustion profile. Obtained details of the parameters (dynamic, total pressures, acoustic amplitudes contours with CH* and OH* fractions etc.) Each fuel simulation outcome based on parameters per Equivalence ratio was analysed and compared. The result enabled the characterisation and combustion instability susceptibility profiling of the fuels**.** DPK/AGO fuels were found to exhibit more stability and lower flammability limits under leaner Equivalence ratios, the hence lesser propensity of combustion instabilities occurrence

**Index Terms**— computational fluid dynamics, Equivalence ratio, combustion instabilities, direct numerical simulation, ANSYS fluent

## 1 INTRODUCTION

The gas turbine happens to be the engine of choice for propulsion and mechanical drives mostly in power generation, aviation the oil and gas as well as the marine industries due to its ruggedness, its ability to operate under any environment, However, the gas turbine is plagued by the combustion instabilities phenomenon which limits its operational availability and reliability.

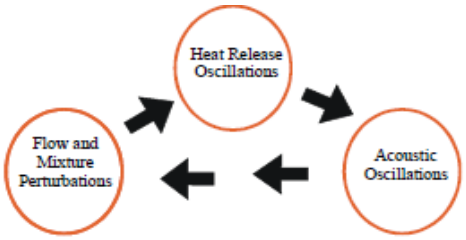


The continuous availability of the gas turbine engine is central to operational efficiencies of many industries who are overly dependent on it for propulsion and mechanical drives. Its non-availability, therefore, contributes significantly to operational cost overruns of power generating plants, oil and gas, marine and aviation industries and this is due to frequent breakdown and the attendant cost of repairs or outright engine replacement. It has been argued in the works of [10], [7] and [3] that, the gas turbines operating under the lean premixed technology are susceptible to the occurrence of a combustion phenomenon known as combustion instabilities amid varying Equivalence ratios. [11] and [12} defined Equivalence ratio for premixed flames as the actual ratio between fuel and an oxidiser divided by the stoichiometric weight ratio. Combustion Instability occurrences in the gas turbines are predicated on lean mixture ranged between $\phi \geq 1$ during combustion. Gas Turbines operating with the non-premixed technologies are known to generate a lot of combustion heat and flame which is germane to the formation of $NO_x$ and other pollutants. These emissions led to the imposition of stringent regulatory measures by environmental regulatory agencies on the gas turbines and other automotive original equipment manufacturers (OEMs). It is these stringent regulatory measures that birthed the development of premixed technology which has as its primary objective of lowering the reaction temperature. [1] stated that Combustion Instability (CI) occur as a consequence of phase syncing of the combustor acoustic waves with the heat release of the oscillatory combustion flowfield leading to high amplitude vibration. The high amplitude vibration leads to system blowoff and flashback that eventually degrades the combustors, guide vanes, turbine blades and the general engine structural frame. [7], however argued that the instabilities arise from the interactions between the combustor's oscillatory flows and heat release and the flow processes manifesting as large amplitude,organized oscillations of the combustor' flowfield (comprising velocity, pressure temperature and the reactants) which generate disturbance that adds energy to the acoustic field when in phase with the pressure oscillations(Figs. 1 and 2). [6] corroborated this description. However, [1] anchored their argument on the nexus between fuel properties, composition and performance of combustion system, chemical kinetics, flame speed, flame size and their relationship to heat release rate, with the attendant flame blowoff and flashback consequences.

Figure 1: Illustration of Feedback Loop responsible for Combustion Instability Source: Lieuwen (2001)

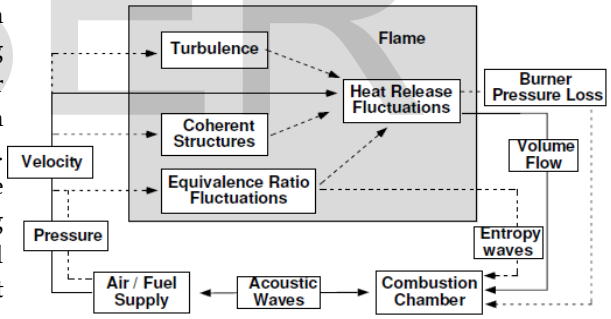


Figure 2. Interactions between flow, acoustics and heat release in a Combustion system. Source: Polifke, (2004)

## 2 MATERIALS AND METHOD

### 2.1 Materials

- ANSYS Fluent (Academic Research CFD) Version 16.2 leveraging on finite difference methods(FDM) to solving the complex Navier-Stoke equation
- The simulation was carried out on an Intel (R) Core (TM) i-3-2377M CPU @ 1.7 GHz, 6BG memory RAM.
- Transient state is calculated until residues lower than $10^{-3}$ for all the variables except for the equation of energy ($<10^{-6}$). A constant time step size (s) of 1 second and numbers of time step of 2500 with 20 max iterations/time step.
- CHEMKIN Collection, Release 3.6 providing gas-phase diffusivities

- GRI-Mech 3.0 Gas-phase kinetic mechanism
- POLIMI Kinetic Mechanism for liquid formation.

## 2.2 Methods

### 2.2.1 Geometric Model Preparation

The Computational Domain (LP combustor) was developed using the AutoCAD software with the following configuration(Figure 3) and exported to the ANSYS Fluent( Academic Research CFD) v.16.2 GUI for meshing (Figures 3 and 4). The model preparation was premised on a geometrical drawing of the combustors and mesh construction, and this played a significant role in the simulation accuracy and the solution convergence through its accuracy and stability of the numerical computation. A 2-D Axis symmetric mesh with 24,834 faces, 12,168 quadrilateral cells of mesh quality of 5.80670e-01 maximum orthogonal skew, and minimum orthogonal quality of 4.13782e-01 was adopted for the simulation. The mesh aspect ratio is 7.26027e+00 (See Figure 4, Tables 1 and 2).The nominal length of the combustor is 800mm, width 200mm, the air and fuel enters into the combustor separately and are premixed by the swirler which is positioned at an angle of 50 degrees to the air and fuel flow. The Swirler is made up of 8 vanes with the following configurations (Fig. 3)

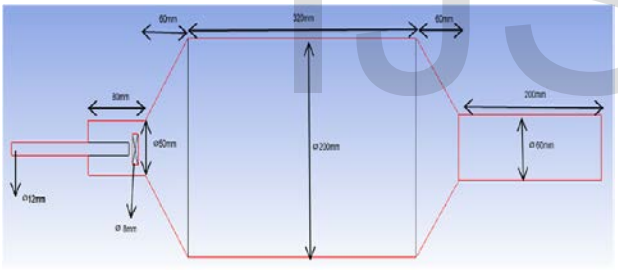


Figure 3: LP Combustor Dimensions

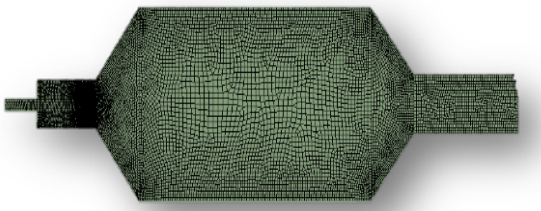

Figure 4. Meshed Layout of the LP Combustor

The simulation process encapsulates the following procedures;

- Designing and applying dimensioning statistics of a typical gas turbine with AutoCAD software to develop the 2-D model with fundamental physics to capture useful results.
- Defining Boundary Conditions – Two inlets (fuel, air), etc., Air mass flow rate, Inlet air temperature, Inlet total pressure of air, Inlet static pressure of air. The mass flow rate of fuel, Inlet fuel temperature, Inlet total pressure of the fuel. The velocity of fuel injection, Outlet Temperature, Pressure loss, combustion efficiency, etc.
- Grid/Mesh Generation
- Analysis Setup – ANSYS Fluent Academic Research CFD v.16.2

Turbulent Model adopted: Turbulent κ-ε model

The entire process entails the execution of series of convoluted DNS of the following fuels 1). Methane($CH_4$) Gas (2). Hydrogen Gas ($H_2$), Gas (3). AGO ($C_{12}H_{24}$) or Diesel fuel (4). Kerosene($C_{12}H_{26}$) or DPK in stepwise procedure on four Equivalence ratios (0.3,0.5,0.7,0.9) that would lead to the determination of the values of the following parameters which are then analysed in series with other to draw or situate the simulation outcome.

i. Dynamic and total pressure magnitudes outlay of fuels at different Equivalence ratios in the computational domain
ii. Fuels temperature profiles at different Equivalence ratios across the computational domain
iii. Fuels mass fractions(OH*, CH* radicals display at various Equivalence ratios within the LP Combustor domain at various Equivalence ratios
iv. Combustion Sound Pressures and Amplitudes of Fuels in different Equivalence ratios across the domain

Table 1: LP Combustor Mesh Generation Statistics

| Method | Triangles | Definitions |
|---|---|---|
| Sizing | Size function = proximity, relevance = fine, smoothing = fine | |
| Volume statistics (m3) | minimum volume (m3): 6.035354e-08, maximum volume (m3): 5.777815e-05 | Total volume (m3): 1.016065e-01 |
| Face area statistics (m2) | minimum face area (m2): 2.008038e-04 maximum face area (m2): 9.971539e-03 | |
| Mesh Quality | Minimum Orthogonal Quality = 4.13782e-01 | Orthogonal Quality ranges from 0 to 1, where values close to 0 correspond to low quality. |
| | Maximum Ortho Skew = 5.80670e-01 | Ortho skew ranges from 0 to 1, where values close to 1 correspond to low quality |
| Maximum Aspect Ratio | 7.26027e+00 | |
| Cells | 12168 | |
| Faces | 24834 | |
| Nodes | 12666 | |

### 2.2.2 Stepwise Procedure

The mass flow rate of air and that of the fuels were predetermined using equations 1 to 5 respectively at an output power of 20000KW(20MW for each fuel type at every Equivalence ratio

$$\dot{m}_{fuel} = {}^{P(KW)}/_{LHV_{fuel}} \text{ X } 1000 \quad (1)$$

$$\dot{m}air = {}^{\dot{m}_{fuel}}/_{MW_{fuel}\phi}/_{MW_{air}Xn_{stoich}} \quad (2)$$

$$\phi = \frac{FAR}{(FAR)_{stoic}} \quad (3)$$

Where

$$FAR = \frac{\dot{m}_{fuel}}{\dot{m}_{air}} \quad (4$$

Stoichiometric combustion equation is shown as follows;

$C_xH_{y+}A\ (O_2 + 3.76N_2) = xCO_2 + ({}^{y}/_{2})H_2{}^{o} + 3.76aN_2$ where a $= x + {}^{y}/_{4}$ and

$$(FAR)_{stoic} = \left(\frac{\dot{m}_{fuel}}{\dot{m}_{air}}\right)_{stoic} = \frac{1}{4.76a}\frac{(MW)_{fuel}}{(MW)_{air}} \quad (5)$$

Where $P$ is the Power output, $LHV_{fuel}$ represent the Lower Heating Value of fuel, $\phi$ is the combustion Equivalence ratio, $n_{air}$ is the mole amount in stoichiometric-fuel-air combustion. The amount of simulations was limited to different premixed air-fuel ratios($\dot{m}_{air}/\dot{m}_{fuel}$) and $MW$ is the molecular weight of fuel.

The obtained values for each fuel per Equivalence ratio were inputted into respective solvers with all set boundary conditions and fuel properties (Table 3)

The Simulations were executed on two fronts taking cognisance of their respective physical dispositions regarding their flow statuses. The inviscid flow/Compressible fuels (Methane and Hydrogen) gas fuels and the liquid fuels which are relatively higher viscosity indices and incompressible (AGO/Diesel and Kerosene(DPK). Due to the physical statuses of the fuels, the Solver was respectively set to pressure-based transient model and the pressure-based Steady model. All fluids, both viscid and inviscid fluids were spark ignited incorporated in the LP combustor. To allow for broad species of combustion reactions, transport model, chemistry interaction –eddy dissipation concept and the volumetric reactions were all coupled with the CHEMKIN format. The CHEMKIN format contains the kinetic reaction mechanisms of the Gas Research Institute (GRI), Gas Fuel Mechanism and the POLIMI Kinetic mechanisms for liquid fuels.

Transient state is calculated until residues lower than $10^{-5}$ for all the variables except for the equation of energy ($<10^{-6}$). A constant time step size (s) of $1e^{-05}$ second and numbers of time step of 200 with 20 max iterations/time step. Flashback was detected during the simulation because of the swirler motion; however, this does not pose any problem to the scope of the simulation.

The next step of the simulation analysis entails the initialisation and the solution control processes within the CFD Solvers. This involves resolution of the discrete values of the flow properties, such properties as velocity, pressure-temperature including other transport parameters which must be initialised within the solver to enable the calculation of the solution to the governing equation. This is because the occurrence within flows is complex and non-linear. Several iteration processes were undertaken earlier to observe simulation consistency and ultimately convergence.

The simulation outcome of both solver modes per each parameter for each fuel was plotted and subsequently read-off and translated into Tables 4-15

Table 2: Simulation Set-up Details

| Models | Function Description of Governing Parameters adopted for the Investigation |
|---|---|
| Solver | Pressure based, absolute velocity formulation, transient time bases simulation |
| Model | $k-\varepsilon$ standard model, Radiation – discrete ordinate, |
| Spark ignition (for gas fuel only) | Initial radius – 0.0002, location – 0.169104, 0.0234036, |
| Acoustic | Broadband noise sources |
| scaled residuals | 10-6 for all the equations |
| species | Transport model, Chemistry interaction – eddy dissipation concept, volumetric reaction coupled with CHEMKIN option to allow for significant species of combustion reactions |
| Kinetics reaction mechanism. | Kinetic reaction mechanism of the Gas Research Institute (GRI) mechanism (Gas fuel), and POLIMI kinetic mechanisms (Liquid fuel) both in CHEMKIN format |
| Scheme | Couple |
| Discretization | Gradient –Least square cell base Pressure - 2nd order Upwind momentum – 2nd order Upwind others – 1st order upwind |
| Solution control | Default |
| Initialization | Standard |
| Calculation | Time step size – 0.00001, numbers of time step = 500, max iteration = 20 |
| Mesh Scale | X-min(mm) -172, X- max(mm) 696 Y-min(mm) -2.8715e-31, Y-max(mm) 198.926 |
| Total Volume(m3) | 1.016065e-01 |
| Face Area Statistics | Minimum face area (m2): 5.090730e-04 Maximum face area(m2): 1.010023e-02 |

Table 3: Properties of Fuels Investigated and Initial Conditions Deployed

| Fuel | Impeller Diameter D (m) | Kinematic Viscosity V @ 15°C M²/S | Rotational Speed N Rev/Sec | Rotational Speed (N * 2π) Rad/Sec | Fuel inlet diameter (m) | Air inlet diameter (m) |
|---|---|---|---|---|---|---|
| Methane | 0.008 | $1.59 \times 10^{-5}$ | 7.95 | 49.95 | 0.015 | 0.10 |
| Hydrogen | 0.008 | $1.01 \times 10^{-4}$ | 50.5 | 317.3 | 0.015 | 0.10 |
| Kerosene | 0.008 | $2.71 \times 10^{-6}$ | 1.355 | 8.513 | 0.015 | 0.10 |
| Diesel | 0.008 | $2.5 \times 10^{-6}$ | 1.25 | 7.853 | 0.015 | 0.10 |

$D = 0.008$, $D^2 = 0.000064$

## 3 RESULTS AND DISCUSSION

### 3.1 Kerosene(DPK)

The Simulation outcome of Kerosene at $0.3\phi$(also referred as Dual-Purpose Kerosene, (DPK) revealed combustion dynamic pressure reduction from the combustion zone from 451.8KPa at combustor inlet to 196kPa at combustor midstream to increase in pressure of 874kPa at 60cm upstream combustion zone. Temperature of 1,044.12K consistency (with fractional variation) was observed throughout the combustor axis. However, the Total pressure readings showed a consistent growth from 351kPa at inlet with a sudden burst to 500kPa at 20cm from combustor inlet through pressure dissipation at 60cm to 371kPa. Dynamic and total pressure observations were found to be significantly lower at $0.5\phi$, $0.7\phi$ and $0.9\phi$ than at $0.3\,\phi$. Total Temperature consistency of 1,044.12K was observed at all Equivalence ratios. (Tables 4-6) The fuel exhibited consistent and marginal temperature fluctuation difference within 0.3ϕ and across Equivalence ratio of an average of 1044K total temperature build up. The dynamic and total pressure build up was highest at 0.3ϕ and lowest at 0.9ϕ and with the highest fluctuation at 0.3ϕ (Tables 4. and 6).

Table 4: Dynamic Pressure Profile across equivalence ratios for DPK Combustion

| Length within Combustor(m) | 0.3φ | 0.5φ | 0.7φ | 0.9φ |
|---|---|---|---|---|
| 0 | 451,852.00 | 165,385.00 | 83,824.00 | 49,455.00 |
| 0.2 | 325,926.00 | 115,385.00 | 60,294.00 | 37,455.00 |
| 0.4 | 196,296.00 | 69,231.00 | 36,029.00 | 22,182.00 |
| 0.6 | 874,074.00 | 315,152.00 | 161,765.00 | 97,455.00 |

Table 5: Total Temperature Profile across Equivalence ratios for DPK Combustion

| Length within Combustor(m) | 0.3φ | 0.5φ | 0.7φ | 0.9φ |
|---|---|---|---|---|
| 0 | 1,044.12 | 1,044.59 | 1,044.41 | 1,042.53 |
| 0.2 | 1,044.59 | 1,044.85 | 1,044.82 | 1,042.94 |
| 0.4 | 1,044.71 | 1,045.15 | 1,045.00 | 1,043.09 |
| 0.6 | 1,044.81 | 1,045.29 | 1,045.18 | 1,043.24 |

Table 6: Total Pressure Profile across Equivalence ratios for DPK Combustion

| Length within Combustor(m) | 0.3φ | 0.5φ | 0.7φ | 0.9φ |
|---|---|---|---|---|
| 0 | 351,852.00 | 130,769.00 | 65,385.00 | 41,818.00 |
| 0.2 | 500,000.00 | 182,051.00 | 93,590.00 | 57,273.00 |
| 0.4 | 388,889.00 | 138,462.00 | 73,077.00 | 43,636.00 |
| 0.6 | 370,370.00 | 312,821.00 | 160,256.00 | 46,364.00 |

### 3.2 Methane/Natural Gas

Pressure observation on methane gas simulation at pressure based steady mode solver at $0.3\phi$ revealed temperature growth from 74kPa through to 124.4kPa (Table 7). There was

however, a decline in dynamic pressure was observed at same Equivalence ratio from 16 kPa to 17.5kPa at regions 0.2m and 0.4m downstream combustor. A sharp rise in pressure to 124kPa occurred at 60cm combustor length. Total temperature characteristics showed gradual temperature increase from 435 k to 3000k occurred at 60cm downstream combustor at 0.3$\phi$. The total pressure readings showed initial total pressure of 158kPa at combustion onset with progressive declination downstream combustor to 84kPa at 40cm and sudden rise to 108kPa at 60cm. (Table 9)

The combustion temperature profile at 0.5$\phi$ showed maximum temperature of 2012.5K occurred at 60cm midstream, and for 0.7$\phi$ occurred at 1823.53k at midstream combustor (60cm) and 1701.70k occurring at 0.9$\phi$ . Experiment conducted by [12] on numerical investigation of the combustion of methane, showed 1850K as the maximum flame temperature, however noted that this value is contrary to the theoretical flame temperature of 1950$^{o}$k obtained under a fast combustion reaction system conducted at initial atmospheric conditions of 100,000k and 200C.

Analysing the temperature differentials within combustor at different Equivalence ratios, revealed through 3000$^{o}$K with a significant temperature difference of 2564.1K at 0.3ϕ, and at 0.5ϕ the fluctuation difference is 1449.5K. The temperature fluctuation difference of methane at 0.7ϕ showed a span of 1235.29K and at 0.9ϕ exhibited 1188.71K differential (Table 8). This observation showed that a coupling (entropy waves) effect is more pronounced at 0.3ϕ (higher temperature and onset of combustion process). Similarly, upstream and downstream dynamic pressure differences across Equivalence ratios equally show it is highest at 0.3ϕ. Combustion pressure across other Equivalence ratios indicates lower upstream pressures than the downstream pressures with Equivalence ratios. (Tables 7 and 9).

Table 7: Dynamic Pressure Profile across Equivalence ratio for Methane Gas Combustion

| Length within Combustor(m) | 0.3φ | 0.5φ | 0.7φ | 0.9φ |
|---|---|---|---|---|
| 0 | 74000 | 77805 | 64783 | 66829 |
| 0.2 | 16000 | 30732 | 27391 | 25366 |
| 0.4 | 17500 | 26098 | 21739 | 17805 |
| 0.6 | 124500 | 72924 | 48696 | 38049 |

Table 8: Total Temperature Profile across Equivalence ratios for Methane Gas Combustion

| Length within Combustor(m) | 0.3φ | 0.5φ | 0.7φ | 0.9φ |
|---|---|---|---|---|
| 0 | 435.9 | 562.5 | 588.24 | 512.99 |
| 0.2 | 1987.18 | 1375 | 1294.12 | 1273.45 |
| 0.4 | 2858.97 | 1589.29 | 1485.29 | 1535.59 |
| 0.6 | 3000 | 2012.5 | 1823.53 | 1701.7 |

Table 9 Total Pressure Profile across Equivalence ratios for Methane Gas Combustion

| Length within Combustor(m) | 0.3φ | 0.5φ | 0.7φ | 0.9φ |
|---|---|---|---|---|
| 0 | 158000 | 190909 | 108205 | 103000 |
| 0.2 | 88000 | 145000 | 57436 | 54000 |
| 0.4 | 84000 | 140000 | 51795 | 48000 |
| 0.6 | 108500 | 9 5000 | 46667 | 70000 |

### 3.3 Automotive Gas Oil/Diesel

The Automotive Gas Oil, otherwise known as diesel oil exhibited the following simulation characteristics during the simulation process conducted at pressure based steady mode setting on the CFD solver. The LP combustion pressure at combustion chamber entry for the 0.3$\phi$ is 400kPa (4bars) declined to 300kPa. It was observed that simulations conducted for further Equivalence ratios compared to 0.3$\phi$ shows decline in combustion dynamic pressure at 0.5φ from 254.3kPa at 60cm downstream combustor length to 15kPa at 20cm at 0.9 φ (Table 7). The total temperature however, exhibited more stability within and across combustors on all Equivalence ratios.

Table 11 shows 1042.69K exhibited at 0.9$\phi$ to a maximum temperature thrust at 1043.84K at 0.7φ. The differential temperature within combustor is 0.88$^{o}$K at 0.3ϕ with a slight fluctuation difference of 0.78K at 0.5 ϕ to 0.63K at 0.9K at 0.9ϕ across all Equivalence ratios simulated. Average Total temperature build of kerosene across all Equivalence ratios is 1042K. However, it was equally observed that the combustion total pressure peaked 766kPa at 0.3$\phi$ within 60cm downstream combustor (Tables 12). The pressure differential across Equivalence ratios is highest at 0.3ϕ upstream with a 360kPa fluctuating difference

Table 10: Dynamic Pressure Profile across Equivalence ratios for AGO fuel Combustion

| Length within Combustor(m) | 0.3φ | 0.5φ | 0.7φ | 0.9φ |
|---|---|---|---|---|
| 0 | 400,000.00 | 127,659.60 | 63,000.00 | 35,714.00 |
| 0.2 | 300,000.00 | 100,000.00 | 49,000.00 | 26,857.00 |
| 0.4 | 195,833.00 | 56,383.00 | 26,000.00 | 15,147.00 |
| 0.6 | 773,529.00 | 254,383.00 | 124,500.00 | 70,000.00 |

Table 11: Total Temperature Profile across Equivalence ratios for AGO Combustion

| Length within Combustor(m) | 0.3φ | 0.5φ | 0.7φ | 0.9φ |
|---|---|---|---|---|
| 0 | 1,043.82 | 1,043.60 | 1,043.22 | 1,042.06 |
| 0.2 | 1,044.41 | 1,044.10 | 1,043.68 | 1,042.69 |
| 0.4 | 1,044.41 | 1,044.21 | 1,043.84 | 1,042.69 |
| 0.6 | 1,044.70 | 1,044.38 | 1,043.84 | 1,042.69 |

Table 12: Total Pressure Profile across Equivalence Ratios AGO Gas Combustion

| Length within Combustor(m) | 0.3φ | 0.5φ | 0.7φ | 0.9φ |
|---|---|---|---|---|
| 0 | 306,666.70 | 100,000.00 | 50,000.00 | 31,023.60 |
| 0.2 | 459,999.00 | 150,000.00 | 72,916.70 | 42,362.20 |
| 0.4 | 333,333.00 | 112,500.00 | 54,166.67 | 35,748.03 |
| 0.6 | 766,666.00 | 252,083.30 | 122,916.70 | 73,385.80 |

### 3.4 Hydrogen Gas

The hydrogen gas exhibited higher total pressure reading at 0.3$\phi$ ranging from 1679.83K at onset combustion process through 1484.03K at 60cm midstream combustor length. The associated temperatures at same Equivalence ratio shows temperature spanning 2000K through 5000K at 60cm combustor. The dynamic pressure reading showed a minimal build from 323.94pa at 20cm combustor length to 1.6kPa (Table 13). Readings exhibited at 0.5$\phi$ and 0.7$\phi$ indicates that the dynamic and total pressure declined relative to 0.3$\phi$ Tables 13 and 15). Total temperatures across combustor at 0.5$\phi$ declined relative to 0.3$\phi$ but remained consistent at 1044K, but with a surge at 0.9$\phi$ across combustor from 1611.11K at 20 cm through 5000$^{o}$K at 60cm upstream combustor. The total pressure readings for 0.7$\phi$ and 0.9$\phi$ shows lower but consistent readings. This fuel showed a temperature growth fluctuation difference of 3000K at 0.3ϕ, remained steady and consistent at 0.5ϕ within combustor (0.78K marginal difference within combustor). This is against that demonstrated at 0.7ϕ, which showed significant difference of 2255.56K within combustor and 2152.17K fluctuation difference at 0.9ϕ(Table 11). This aptly demonstrate temperature fluctuation decline with increasing Equivalence ratio with highest dynamic and total pressure at 0.3ϕ with significant decrease with increasing Equivalence ratio.

Table 13: Dynamic Pressure Profile across Equivalence ratios for Hydrogen Gas Combustion

| Length within Combustor(m) | 0.3φ | 0.5φ | 0.7φ | 0.9φ |
|---|---|---|---|---|
| 0 | 323.94 | 97.44 | 88.24 | 94.57 |
| 0.2 | 204.23 | 79.49 | 47.06 | 38.04 |
| 0.4 | 218.31 | 89.74 | 57.35 | 44.57 |
| 0.6 | 1,661.97 | 669.23 | 379.41 | 263.04 |

Table 14: Total Temperature Profile across Equivalence ratios hydrogen gas combustion

| Length within Combustor(m) | 0.3φ | 0.5φ | 0.7φ | 0.9φ |
|---|---|---|---|---|
| 0 | 2,000.00 | 2,500.00 | 2,744.44 | 2,847.83 |
| 0.2 | 2,288.89 | 3,628.21 | 1,611.11 | 4,760.89 |
| 0.4 | 5,000.00 | 5,000.00 | 5,000.00 | 5,000.00 |
| 0.6 | 5,000.00 | 5,000.00 | 5,000.00 | 5,000.00 |

Table 15: Total Pressure profile across Equivalence ratios hydrogen gas combustion

| Length within Combustor(m) | 0.3φ | 0.5φ | 0.7φ | 0.9φ |
|---|---|---|---|---|
| 0 | 1,679.83 | 1043.6 | 429.63 | 337.78 |
| 0.2 | 1,542.02 | 1044.1 | 379.63 | 272.22 |
| 0.4 | 1,400.00 | 1044.21 | 381.48 | 274.44 |
| 0.6 | 1,484.03 | 1044.38 | 388.89 | 266.67 |

### 3.5 Findings

#### 3.5.1 Methane Gas

The flame temperature of methane gas taken along combustor axis at midstream (reaction zone) at 0.5$\phi$(2012K) 0.7$\phi$(1823.53K) and 0.9$\phi$(1701.70K) are in the range with the works of [12] whose works on "*Numerical Investigation of the combustion of methane-air in Gas Turbine Can-Type Combustion Chamber*" revealed maximum flame temperature at 1850K (adiabatic temperature) who posited that theoretical flame temperature produced by flame with a fast combustion reaction is 1950K

#### 3.5.2 Kerosene(DPK) Fuel

The Kerosene(DPK) fuel was observed to exhibit consistency in a flame temperature range of 1042.53-1045.15K at all Equivalence ratios. This amply suggests moderate stability in the flame temperature range for DPK. These high temperatures were observed in the combustor reaction zone along the combustor axis (up to 60cm combustor length).

#### 3.5.3 Hydrogen Gas

The flame temperature ranges between 2000k at 0.3$\phi$ and 5000k at 0.9$\phi$ which depicts increase as the Equivalence ratios increase. The magnitude of the temperature is synonymous with increase Equivalence ratios and mass fraction. The findings here align with that of [12] who worked on the relationship between flame length, temperatures and mass fraction magnitudes

#### 3.5.4 Automotive Gas Oil/Diesel Fuel

The Automotive Gas Oil(Diesel) demonstrated a consistent temperature profile range of (1042.49-1043.82) K across all Equivalence ratios at the combustor's reaction zone. The findings on compressible fluids (Methane and Hydrogen gases) are similar, so also the incompressible fluids (Automotive Gas Oil and Kerosene). Few works are reported

in the literature on the impact of fuel types on combustion instabilities. The work of Pathan et al. [12] on methane combustion provides credence to this work.

## 4 CONCLUSION

It was observed from the dynamic and total pressures readings that the incompressible liquid fuels- Kerosene and AGO, showed higher combustible dynamic pressures than the compressible gaseous fuels at a lower Equivalence ratio at 0.3 ϕ with pressures reducing upstream combustor and a sudden spike in pressure at the most upstream. Another observation is decreasing pressures with increasing Equivalence ratios.

Total temperature profile at 0.3ϕ exhibited that the incompressible liquid fuels displayed higher and steadier temperature profile through the combustor, with methane gas fuel posting the most temperature spikes across combustor. The hydrogen fuel showed the highest temperature profile across all fuels staggered across 0.5, ϕ 0.7 ϕ and 0.9 ϕ. The Hydrogen and methane gases showed apparent consistent profiles with early and single spikes across all Equivalence ratios

The above simulation findings ably aptly demonstrated the effect of Equivalence ratio fluctuations on various fuels during combustion instabilities in gas turbine engines, while further providing a detailed characterisation of all the four fuels used for the study, as various combustion pressure and temperature details were obtained for each fuel. Combustion instability is the consequence of the positive coupling of the combustor excited acoustic field with the unsteady heat release of the flame during unstable combustion processes. The unsteady heat release must be in phase with the acoustic-pressure- a condition necessary for energy addition to the unsteady motions [5]; [3]; [10]; [7]; [13]; [4]; [14].

The main precipitance of combustion instability and combustion noise is credited to the application of the LP Combustor to lower combustion temperatures, a process encouraged by the premixing of the fuel and the oxidiser. [8], [1], [11], [16] stated that the highest temperatures during combustion are obtained upstream combustor (near nozzle), and hydrogen gas temperature was 2330K and the natural gas 2290k. On the other hand, [12] in their work obtained 1850K and had argued against the theoretical temperature of 1950k. The various temperature profiles as obtained by this study showed explicitly what was obtainable at various Equivalence ratios and correlates with the work of [16] and [12]

This work detailed the maximum temperature and pressures obtainable with each fuel and at what Equivalence ratio they were obtained. [15] in their work stated that the gas turbine exhaust temperatures hoover around 2073.15K-2273.15K, which they considered too hot for the nozzle guide vanes of the turbine.[2] argued that in reference to the Zeldovich equations for thermal $NO_x$ that $NO_x$ is generated to the limit of available oxygen at about 200,000ppm at temperatures above 1573.5K and that no $NO_x$ is produced at a temperature below 1033.15K.

## ACKNOWLEDGMENT

Profound gratitude to BSN Nigeria allowing the use of the facility for private research and write-ups.

## REFERENCES

[1] W.A. Chishty, and M. Klein, "Combustion and Emission issues in Gas Turbines". http://www.iagtcommittee.com/downloads/2009papers/Training%20Session2%20-%20Combustion%20Issues%20in%20Gas%20Turbines. 2009.

[2] Clean Air Technology Centre, "Nitrogen Oxides(NOx), Why and How they are Controlled", EPA Technical Bulletin 456/F-99-006R November. 1999.

[3] F.C Culick, and V. Yang, "Overview of Combustion Instabilities in Liquid - Propelled Rocket Engines". http://core.ac.uk/download/pdf/4886871.pdf. 1995.

[4] F.C. Culick, "Combustion instabilities in liquid-fueled propulsion systems", *Paper reprinted from conference proceedings No. 450 Advisory Group for Aerospace Research & Development AGARD*. http://www. authors.library.caltech.edu/22028 /. 2012

[5] A. Dowling, "The Calculations of Thermoacoustic Oscillations". *Journal of Sound and Vibrations* (1995) 180(4), 557-58

[6] S. Ducruix, T. Schuller, D. Durox, and S. Candel, "Combustion Instability Mechanisms in Premixed Combustors". *Combustion Instabilities in Gas Turbine Engines: Operational Experience, Fundamental Mechanisms and Modelling*. T. Lieuwen and V. Yang eds., Progress in Aeronautics and Aeronautics Series, Vol. 210. AIAA, pp.179-212, 2005

[7] T. Lieuwen, "Investigation of Combustion Instability Mechanisms in Lean Premixed Gas Turbines". PhD Thesis, Dept. of Mechanical Engineering. Georgia Institute of Technology Georgia, California.1999

[8] T. Lieuwen, H. Torres, C. Johnson, and B. Zinn, "A Mechanism of Combustion Instability in Lean Premixed Gas Turbine Combustors" *Journal of Engineering for Gas Turbines and Power*, Vol. 123, No 1, 2001, pp.182-190. 2001.

[9] T. Lieuwen, "Modelling Premixed Combustion-Acoustic Wave Interactions: A review". *Journal of Propulsion and Power Vol. 19, No 5 September-October 2003*.

[10] T. Lieuwen and B.T. Zinn, "The Role of Equivalence Ratio Oscillations in Driving Combustion Instabilities in Low NOx Gas Turbines". *Proceedings of the Combustion Institute, Vol 27, The Combustion Institute Inst., Pittsburgh, PA*, pp. 1809-1816. 1998

[11] L. Merotto, M. Sirignano, M. Commodo, A. D'Anna, R. Donde, and S. De luliis, "Experimental Characterization and Modelling for Equivalence Ratio Sensing in Non-Premixed Flames using Chemiluminescence and Laser-Induced Breakdown Spectroscopy Techniques". Energy Fuels, 2017, 31 (3), pp 3227–3233.

[12] F.H. Pathan, N.K Patel and M.V. Tadvi, "Numerical Investigation of the Combustion of the Methane-Air Mixture in Gas Turbine Can-Type Combustion Chamber". *International Journal of Scientific & Engineering Research*. Volume 3, Issue10, October-2012 ISSN-2229-5518.

[13] W. Polifke, "Combustion instabilities". *VKI Lecture Series Journal of Advances in Acoustics and Applications* March 15th – 19th, Brussels Belgium

[14] S. Pawar, A. Seshadri, V. Unni and R. Sujith "Thermoacoustic Instability as Mutual Synchronisation between the Acoustic Field of the Confinement and Turbulent Reactive Flow" Journal *of Fluid Mechanics.Vol.*827, pp.664-693. 2017 doi:10.1017/jfm.2017.438

[15] A. Trifan and A. Pruiu "Technologies used on Maritime Boilers for the Reduction of NOx Emissions". Bulletin of the Transilvania University of Brasov. Vol. 2(51)-2009 Series 1: Engineering Sciences. 2010

[16] H. Tomczak, G. Benelli, L. Carai and D. Cecchini "Investigation of A Gas Turbine Combustion System Fired with Mixtures of Natural Gas and Hydrogen". *IFRF Combustion Journal, Dec. 2002*, 19 pp. Article ID 200207

[17] D. You, V. Yang and X. Sun (2003). "Three-Dimensional Linear Stability Analysis of Gas Turbine Combustion Dynamics" T. Lieuwen, and V. Yang eds., *Combustion Instabilities in Gas Turbine Engines: Operational Experience, Fundamental Mechanisms and Modelling*. Progress in Aeronautics and Aeronautics Series, Vol. 210. AIAA. 417-448. 2005

**Authors**

- **Wilson Alli is currently pursuing doctorate programme in Mechanical Engineering Department Ambrose Alli University, Ekpoma Edo State Nigeria Phone: +234(0)8080175708. Email: wilsalli@gmail.com**

- **Prof. Osagie Ighodalo is of the Mechanical Engineering Department Ambrose Alli University, Ekpoma Edo State Nigeria. Phone: +234(0)8033626385. Email: oighodalo@yahoo.com**

- **Prof. Christopher Ajuwa is of the Mechanical Engineering Department Federal University of Petroleum Resources Effurun-Warri Delta State Nigeria Phone: +234(0)8055515958. Email: ajuwachris@yahoo.com**